Title

3D T1rho sequences with FASE, UTE, and MAPSS acquisitions for knee evaluation

Journal

Japanese Journal of Radiology, 41(11)

ISSN

1867-1071

Authors

Bae, Won C

Malis, Vadim

Kassai, Yoshimori

et al.

Publication Date

2023-11-01

DOI

10.1007/s11604-023-01453-8

3D T1rho Sequences with FASE, UTE, and MAPSS Acquisitions for Knee Evaluation

Won C. Bae,[1,2] PhD; Vadim Malis,[1] PhD; Yoshimori Kassai,[4] MS; Mitsue Miyazaki,[1] PhD;

[1,3] Won C. Bae, PhD	wbae@health.ucsd.edu
[1] Vadim Malis, PhD	vmalis@ucsd.edu
[2] Yoshimori Kassai, MS	yoshimori.kassai@medical.canon
[1] Mitsue Miyazaki, PhD	mimiyazaki@health.ucsd.edu

1. Department of Radiology, University of California-San Diego, La Jolla, CA
2. Canon Medical Systems, Tochigi, Japan
3. Department of Radiology, VA San Diego Healthcare System, San Diego, CA

Corresponding author:
Won C. Bae, PhD
Department of Radiology
University of California, San Diego
9427 Health Sciences Drive
La Jolla, CA 92093-0997
TEL: (858) 246-2240
email: wbae@health.ucsd.edu

Submitted to: Skeletal Radiology

Manuscript Type: Technical Report

KEYWORDS

MRI, osteoarthritis, cartilage, meniscus

ACKNOWLEDGMENT

Research reported in this publication was supported in parts by grants from Canon Medical Systems USA and National Institute of Arthritis and Musculoskeletal and Skin Diseases P30 AR073761 to Dr. Bae, and grants from Canon Medicals System USA and Canon Medical Systems Corporation to Dr. Miyazaki. Dr. Kassai is an employee of Canon Medical Systems Corporation. The content of this work is solely the responsibility of the authors and does not necessarily represent the official views of the sponsoring institutions.

3D T1rho Sequences with FASE, UTE, and MAPSS Acquisitions for Knee Evaluation

ABSTRACT

Purpose: For biochemical evaluation of soft tissues of the knee, T1rho magnetic resonance imaging (MRI) has been proposed. Purpose of this study was to compare three T1rho sequences based on fast advanced spin echo (FASE), ultrashort echo time (UTE), and magnetization-prepared angle-modulated partitioned k-space spoiled gradient echo snapshots (MAPSS) acquisitions for the knee evaluation.

Materials and Methods: We developed two T1rho sequences using 3D FASE or 3D radial UTE acquisitions. 3D MAPSS T1rho was provided by the manufacturer. Agarose phantoms with varying concentration were imaged. Additionally, bilateral knees of asymptomatic subjects were imaged sagittally. T1rho values of the phantoms and 4 regions of interest (ROI) of the knees (i.e., anterior and posterior meniscus, femoral and tibial cartilage) were determined.

Results: In phantoms, all T1rho values monotonically decreased with increasing agarose concentration. 3D MAPSS T1rho values of 51, 34, and 38 ms were found for 2%, 3%, and 4% agarose, respectively, similar to published values on another platform. In the knee, the raw images were detailed with good contrast. Cartilage and meniscus T1rho values varied with pulse sequence, being the lowest in the 3D UTE T1rho sequence. Comparing different ROIs, menisci generally had lower T1rho values compared to cartilage, as expected in healthy knees.

Conclusion: We have successfully developed and implemented the new T1rho sequences and validated them using agarose phantoms and volunteer knees. All sequences were optimized to be clinically feasible (~5 min or less) and yielded satisfactory image quality and T1rho values consistent with the literature.

INTRODUCTION

Osteoarthritis (OA) of the knee is a significant health concern involving articular cartilage injury and degeneration, resulting in high morbidity and diminished quality of life, along with a high socioeconomic cost [1]. Due to excellent soft tissue contrast, magnetic resonance (MR) imaging is a popular imaging modality for the evaluation of cartilage disease and knee OA. Clinically, MR imaging of the knee focuses on morphologic abnormalities using appropriate imaging sequences to alter the image contrast. However, even in the setting of minimal morphologic changes, damages to the major constituents of this tissue (i.e., collagen and proteoglycan) can indicate a degenerative progression.

For biochemical evaluation of articular cartilage, quantitative MRI techniques such as T2 and T1rho mapping have been developed. T1rho relaxation, in particular, describes spin-lattice relaxation in the rotating frame in the presence of an external spin-lock radiofrequency (RF) pulse in the transverse plane. In vitro studies, T1rho values of cartilage have been shown to be sensitive to biochemical content [2-4], where higher T1rho values correlate with lower PG content, associating with knee OA [5].

T1rho sequences are typically implemented using preparation spin-lock RF pulses followed by a variety of acquisition sequences. T1rho acquisition based on 3D magnetization-prepared angle-modulated partitioned k-space spoiled gradient-echo snapshots (3D MAPSS) [6, 7] is arguably most widely available, implemented on multiple vendor platforms (i.e., Siemens, General Electric, and Philips) as research sequences. Here, T1rho preparation with continuous spin-lock pulses with 180 degree phase shift in the 2nd half is used, followed by a gradient crusher, image acquisition, and a delay for magnetization restoration. For MAPSS acquisition,

multiple k-space lines are acquired after each T1rho preparation, often in an interleaved segmented elliptic-centric trajectory (i.e., square spiral).

T1rho sequences using other types of acquisition sequences are less common but available. T1rho CubeQuant [8] utilizes a 3D fast spin echo acquisition in a signal-to-noise (SNR) efficient manner. Gradient recalled echo (GRE) [9] and balanced GRE [10] have also been used for image acquisition. T1rho imaging with single shot fast spin echo or fast advanced spin echo (FASE) has been reported for liver [11] but not musculoskeletal (MSK) applications, although FASE offers advantages of high SNR and short scan time. For MSK tissues with intrinsically short T2 properties such as cortical bone, osteochondral junction, tendons and ligaments, etc., T1rho sequences utilizing ultrashort echo time (UTE) or zero echo time (ZTE) acquisition has been developed [12-16], and have shown that T1rho value are useful biomarker for changes in biochemical [14] and biomechanical [17] properties of MSK tissues.

There is not one T1rho sequence that is considered the gold standard when it comes to T1rho imaging of the knee. Human knee is also complicated in that tissues with long (synovial fluid, fat, muscle) and short (bone, ligament, meniscus) T2 properties co-exist and need to be evaluated together. For T2 and T2* evaluation, different quantitative sequences using spin echo, gradient echo, and ultrashort echo time exist to target different tissues. Additionally, it is imperative clinically that similar types of quantitative techniques provide consistent values. Development of multiple sequences for T1rho MRI is important for the similar reason, to ensure consistency and to target various tissues with inherently different MR properties.

The purpose of this early study was to compare three T1rho sequences newly implemented on the Canon platform, utilizing T1rho preparation spin-lock RF pulses followed

by three different acquisition sequences of 3D fast advanced spin echo (FASE), 3D ultrashort echo time (UTE), and 3D MAPSS, acquired on agarose phantoms as well as knees of asymptomatic volunteers.

MATERIALS AND METHODS

This study involving human subjects was approved by the institutional review board (*#blinded for review*) and written consent was obtained from each participant.

Phantoms and Human Subjects

Agarose Phantoms: The agarose phantoms consisted of 45 ml of agarose gel placed in 50ml plastic centrifuge tubes. The phantoms had an agarose concentration (w/w) of the 2%, 3%, and 4%, respectively, as described previously [18], and were scanned at room temperature.

Human Subjects: Bilateral knees of 5 asymptomatic volunteers (4 male, 1 female, ages 31 to 66 years old) were included for 3D FASE and 3D UTE imaging, and a subset of 3 volunteers (2 male, 1 female, ages 49 to 66 years) were included for 3D MAPSS imaging.

Magnetic Resonance Imaging

MR imaging was performed on a clinical 3-Tesla (Vantage, Galan 3T, Canon Medical Systems Corp., Japan) scanner using a 16-channel transmit and receive knee coil. Phantoms were imaged transversely. Knees were imaged sagittally covering lateral and medial compartments.

The following T1rho sequences were used, each with a preparation pulse (Figure 1A) containing continuous spin-lock pulses with 180 degrees phase shift in the 2nd half, followed by a gradient crusher. For image acquisition, the first T1rho sequence was 3D FASE (a.k.a. 3D single-shot fast spin echo) (Figure 1B), permitting volumetric acquisition using isotropic voxels, allowing high-resolution re-slicing from any desired direction, useful for the complex knee anatomy requiring examination in multiple planes. The 2nd sequence was 3D radial UTE (Figure 1B) acquisitions, with the ability to use echo time as low as 0.096 ms to enable acquisition of MR signal from many short T2 MSK tissues. The 3rd sequence was 3D MAPSS (Figure 1C), which is a prototype of QIBA compliant compatible sequence provided from the manufacturer, and similar in k-space trajectory as those implemented on other vendor platforms. Table 1 shows the detailed scanning parameters for each T1rho sequence.

Image Analysis

For phantom data, a central axial slice was chosen, and circular regions of interest (ROI) were placed in the center of each agarose phantom to determine the mean T1rho value. T1rho color maps (Figure 2, color) were also created. For the human knees, sagittal slices in the lateral and medial weight bearing compartments were selected and four ROIs (Figure 5, color) of femoral cartilage (FC), tibial cartilage (TC), anterior meniscus (AM), and posterior meniscus (PM) were drawn manually to determine the respective T1rho values.

For T1rho fitting, within each ROI, signal intensity of all voxels was averaged and fit (Figure 3) using a nonlinear least square fitting routine in Matlab to a simple mono-exponential

decay function (Equation 1) where S(TSL) is the mean signal intensity at different spin lock times (TSL), S_0 and T1rho are fitted parameters.

$$S(TSL) = S_0 \exp\left(TSL \,/\, T1rho\right) \qquad (1)$$

Statistics

For the knee evaluation, descriptive statistics including mean and standard deviation (of all subjects) for were calculated for each region of interest. In addition, effect of pulse sequence on the mean T1rho values was compared using ANOVA with Tukey post-hoc test, with the significance level set at 0.05. For each individual pulse sequences, effect of region of interest on T1rho value was determined also using ANOVA. As an additional way to show differences between T1rho values from the three sequences, we performed Bland-Altman analysis.

RESULTS

Agarose Phantom

Figure 2 shows selected raw images of agarose phantoms imaged with the three T1rho sequences, along with T1rho colormaps. General trends of decreasing signal intensity with increasing spin lock times (TSL) and decreasing T1rho values with increasing agarose concentration was observed. Figure 3 shows T1rho curve-fits for the 2% agarose phantom, suggesting good tight fits for all three techniques. Figure 4 shows the T1rho values of the phantoms confirming the decreasing trend with increasing agarose concentration, suggesting that the sequences were sensitive to macromolecular content. While the T1rho values from the three sequences were not identical, there were within a reasonable range (~5 ms) from each

other, and the values for the UTE sequence tended to be lower than those from other sequences.

Human Knees

Figure 4 shows selected raw images of the knee imaged with the three T1rho sequences (Figure 4ACE) along with colormaps (Figure 4BDF) of the four ROIs in the cartilage and the menisci. The raw images were detailed and artifact-free in the ROI and showed decreasing signal intensity of cartilage and meniscus with increasing TSL.

Table 3 shows mean and standard deviation of the T1rho values measured on the four ROIs using the three pulse sequences. T1rho values varied significantly ($p<0.000001$) with pulse sequence; T1rho values from the 3D UTE sequence (mean of 22.1 to 26.8 ms in different ROIs) were significantly lower than those from other sequences (post-hoc $p<0.00001$ each; mean of 24.7 to 37.9 ms). Comparing different ROIs, both 3D FASE (ANOVA $p=0.03$) and 3D MAPSS ($p<0.00001$) suggested significant differences between ROIs; in general, the menisci had lower T1rho values (mean of 24.7 to 29.7 ms) compared to the cartilage (29.1 to 37.9 ms). T1rho values from 3D UTE sequence showed similar trends but this was not statistically significant ($p=0.25$).

Figure 5 shows Bland-Altman plots for overlapping subjects (since MAPSS was performed only on a subset of 3 subjects) comparing T1rho values of cartilage and meniscus from the three sequences. Between 3D MAPSS and 3D FASE (Figure 5A), the bias was very little (1 ms), although the limits of agreement was large (~20 ms). Between 3D UTE and 3D FASE (Figure 5B), and between 3D UTE and 3D MAPSS (Figure 5C), there was a significant bias of

approximate -7 ms, and similarly large limits of agreement ~20 ms.

DISCUSSION

This was an early study to determine if the T1rho sequences provided reasonable data with T1rho values of the agarose phantoms and normal knees, and if there were differences in the obtained values due to the sequence. Qualitatively, overall image quality (Figure 4) was good, providing images with good contrast and high resolution sufficient to distinguish different tissue components, including articular cartilage and the meniscus. The relaxometry data (Figure 3) also appeared good, providing very tight fitting for the range of TSL used.

Quantitative results for the agarose phantoms were in good agreement with past studies. In particular, our 3D MAPSS sequence yielded T1rho values of 51, 34, and 28 ms for 2%, 3%, and 4% agarose phantoms, respectively, which was close to published values of 54, 39, and 29 ms found in a different platform using a similar 3D MAPSS T1rho acquisition [18]. For T1rho sequences based on UTE or FASE acquisitions, there is little data on T1rho values of agarose. Nonetheless all of the sequences yielded the same trends decreasing T1rho values with increasing agarose concentration.

Quantitative results for the subject knees were also in line with the past results. Table 3 showed that the mean T1rho values of the cartilage (29-38 ms) were generally higher than those of the menisci (25 to 30 ms), as expected in healthy knees. For 3D FASE and 3D MAPSS sequences, the mean T1rho values of the cartilage (29-38 ms in this study) were in the similar range as those reported previously [19-21], while the meniscus T1rho values (25-30 ms) were a little high compared to past reports (15-20 ms) [19-21]. For 3D UTE T1rho, while no direct

comparison is available, compared to other similar sequences such as 3D UTE Cones T1rho [22, 23], our UTE T1rho values of cartilage (~26 ms) were somewhat lower, and the values of the menisci (~22 ms) were similar to, the reported values.

Possible reasons for the discrepancy between T1rho measurements among the three pulse sequences may include different TR/TEs (1497/10 ms, 3.7/0.096 ms, and 6.0/2.8 ms for FASE, UTE, and MAPSS, respectively), TSL, as well as nature of each sequence, such as a spin-echo type for FASE, an ultrashort echo time gradient-echo for UTE sequence, and a regular gradient echo for MAPSS. Bland-Altman plots (Figure 5) also showed a fairly large discrepancy between measurements, and this may be attributable to variations in regions of interest selected on images from the different sequences. We have considered post-processing to register the images but the consequence of this on T1rho calculation was not clear. However, their average values on the phantom and human knee studies are close enough to be used in clinical examinations and showed sensitivity to different concentrations of macromolecules in agarose phantoms. Variations in T1rho values with pulse sequence requires further investigation.

There are several shortcomings of this study. We utilized a single phantom and a relatively small number (3 to 5) of subjects, which may have contributed to some of the discrepancy in T1rho values between this study compared to the literature. This was an early feasibility study, and full validation of reproducibility of each sequence will need to be performed prior to a wide use clinically. Additionally, dependence of T1rho value on the TSL selection and other preparation and acquisition parameters has not been performed. Based on the cartilage T1rho values in literature of around 30 to 40 ms, the present range of TSL (4 to 6

points up to TSL of 80 ms) appeared reasonable. Our study had a single reader for ROI placement, so that is yet another shortcoming that could be addressed. Lastly, we did not have subjects with knee osteoarthritis to test the sensitivity of the sequences to knee OA. We will address this in a larger study in the future.

Each sequence has advantages and disadvantages. We developed the 3D UTE T1rho with radial acquisition for targeting short T2 tissues in the body and the knee, including the deep and calcified layers of articular cartilage [24], ligaments and tendons [25], and cortical bone [26, 27]. In such short T2 tissues, a non-UTE type sequence is unable to capture any signal regardless of T1rho preparation. 3D MAPSS and 3D FASE are both targeted at longer T2 tissues. Both use Cartesian sampling but 3D MAPSS uses a centric ky-kz trajectory as shown in Figure 1C, whereas 3D FASE uses a straight k-space trajectory using each slice encoding followed by phase encoding as shown in Figure 1D. While 3D MAPSS T1rho is an established sequence on multiple vendors that has been studied the most. It uses spoiled gradient echo snapshots acquisition, making it prone to susceptibility artifacts. 3D FASE T1rho is relatively new but has potential advantage in terms of freedom of parameter selection to achieve significant scan time reduction while retaining image quality. But it is prone to blurring due to long echo train length. These characteristics may have contributed to visual differences in the raw MR images. On phantoms (Figure 2) both 3D FASE and 3D UTE gave sharp images, whereas 3D MAPSS shows blurriness. This might be due to reduced matrix in 3D MAPSS readout than that used in FASE and UTE.

In conclusion, we have successfully developed and implemented the two new T1rho sequences using 3D FASE and 3D UTE acquisitions and tested them along with a manufacturer's

3D T1rho MAPSS sequence on agarose phantoms and volunteer knees. All sequences were optimized to be clinically feasible (~5 min or less) and yielded robust and consistent results in line with past studies on similar sequences. Future studies will include rigorous evaluation of parameter-dependence, repeatability, and additional cohorts of subjects.

5

REFERENCES

1. Safiri S, Kolahi AA, Smith E, Hill C, Bettampadi D, Mansournia MA, et al. Global, regional and national burden of osteoarthritis 1990-2017: a systematic analysis of the Global Burden of Disease Study 2017. Ann Rheum Dis. 2020; 79(6):819-828.
2. Duvvuri U, Reddy R, Patel SD, Kaufman JH, Kneeland JB, Leigh JS. T1rho-relaxation in articular cartilage: effects of enzymatic degradation. Magn Reson Med. 1997; 38(6):863-867.
3. Menezes NM, Gray ML, Hartke JR, Burstein D. T2 and T1rho MRI in articular cartilage systems. Magn Reson Med. 2004; 51(3):503-509.
4. Wheaton AJ, Dodge GR, Elliott DM, Nicoll SB, Reddy R. Quantification of cartilage biomechanical and biochemical properties via T1rho magnetic resonance imaging. Magn Reson Med. 2005; 54(5):1087-1093.
5. Schooler J, Kumar D, Nardo L, McCulloch C, Li X, Link TM, et al. Longitudinal evaluation of T1rho and T2 spatial distribution in osteoarthritic and healthy medial knee cartilage. Osteoarthritis Cartilage. 2014; 22(1):51-62.
6. Li X, Wyatt C, Rivoire J, Han E, Chen W, Schooler J, et al. Simultaneous acquisition of T1rho and T2 quantification in knee cartilage: repeatability and diurnal variation. J Magn Reson Imaging. 2014; 39(5):1287-1293.
7. Li X, Han ET, Busse RF, Majumdar S. In vivo T(1rho) mapping in cartilage using 3D magnetization-prepared angle-modulated partitioned k-space spoiled gradient echo snapshots (3D MAPSS). Magn Reson Med. 2008; 59(2):298-307.

8. Jordan CD, McWalter EJ, Monu UD, Watkins RD, Chen W, Bangerter NK, et al. Variability of CubeQuant T1rho, quantitative DESS T2, and cones sodium MRI in knee cartilage. Osteoarthritis Cartilage. 2014; 22(10):1559-1567.
9. Borthakur A, Wheaton A, Charagundla SR, Shapiro EM, Regatte RR, Akella SV, et al. Three-dimensional T1rho-weighted MRI at 1.5 Tesla. J Magn Reson Imaging. 2003; 17(6):730-736.
10. Witschey WR, Borthakur A, Elliott MA, Fenty M, Sochor MA, Wang C, et al. T1rho-prepared balanced gradient echo for rapid 3D T1rho MRI. J Magn Reson Imaging. 2008; 28(3):744-754.
11. Chen W, Chan Q, Wang YX. Breath-hold black blood quantitative T1rho imaging of liver using single shot fast spin echo acquisition. Quantitative imaging in medicine and surgery. 2016; 6(2):168-177.
12. Du J, Carl M, Diaz E, Takahashi A, Han E, Szeverenyi NM, et al. Ultrashort TE T1rho (UTE T1rho) imaging of the Achilles tendon and meniscus. Magn Reson Med. 2010; 64(3):834-842.
13. Mahar R, Batool S, Badar F, Xia Y. Quantitative measurement of T2, T1rho and T1 relaxation times in articular cartilage and cartilage-bone interface by SE and UTE imaging at microscopic resolution. J Magn Reson. 2018; 297:76-85.
14. Chang EY, Campos JC, Bae WC, Znamirowski R, Statum S, Du J, et al. Ultrashort Echo Time T1rho Is Sensitive to Enzymatic Degeneration of Human Menisci. J Comput Assist Tomogr. 2015.

15. Athertya JS, Ma Y, Masoud Afsahi A, Lombardi AF, Moazamian D, Jerban S, et al. Accelerated Quantitative 3D UTE-Cones Imaging Using Compressed Sensing. Sensors (Basel). 2022; 22(19).
16. Sharafi A, Baboli R, Chang G, Regatte RR. 3D-T(1rho) prepared zero echo time-based PETRA sequence for in vivo biexponential relaxation mapping of semisolid short-T(2) tissues at 3 T. J Magn Reson Imaging. 2019; 50(4):1207-1218.
17. Bae WC, Biswas R, Statum S, Sah RL, Chung CB. Sensitivity of quantitative UTE MRI to the biomechanical property of the temporomandibular joint disc. Skeletal Radiol. 2014; 43(9):1217-1223.
18. Buck FM, Bae WC, Diaz E, Du J, Statum S, Han ET, et al. Comparison of T1rho measurements in agarose phantoms and human patellar cartilage using 2D multislice spiral and 3D magnetization prepared partitioned k-space spoiled gradient-echo snapshot techniques at 3 T. AJR Am J Roentgenol. 2011; 196(2):W174-179.
19. Li X, Pedoia V, Kumar D, Rivoire J, Wyatt C, Lansdown D, et al. Cartilage T1rho and T2 relaxation times: longitudinal reproducibility and variations using different coils, MR systems and sites. Osteoarthritis Cartilage. 2015; 23(12):2214-2223.
20. Knox J, Pedoia V, Wang A, Tanaka M, Joseph GB, Neumann J, et al. Longitudinal changes in MR T1rho/T2 signal of meniscus and its association with cartilage T1p/T2 in ACL-injured patients. Osteoarthritis Cartilage. 2018; 26(5):689-696.
21. Kim J, Mamoto K, Lartey R, Xu K, Nakamura K, Shin W, et al. Multi-vendor multi-site T1rho and T2 quantification of knee cartilage. Osteoarthritis Cartilage. 2020; 28(12):1539-1550.

22. Ma YJ, Carl M, Searleman A, Lu X, Chang EY, Du J. 3D adiabatic T(1rho) prepared ultrashort echo time cones sequence for whole knee imaging. Magn Reson Med. 2018; 80(4):1429-1439.
23. Wu M, Ma YJ, Kasibhatla A, Chen M, Jang H, Jerban S, et al. Convincing evidence for magic angle less-sensitive quantitative T(1rho) imaging of articular cartilage using the 3D ultrashort echo time cones adiabatic T(1rho) (3D UTE cones-AdiabT(1rho)) sequence. Magn Reson Med. 2020; 84(5):2551-2560.
24. Bae WC, Dwek JR, Znamirowski R, Statum SM, Hermida JC, D'Lima DD, et al. Ultrashort echo time MR imaging of osteochondral junction of the knee at 3 T: identification of anatomic structures contributing to signal intensity. Radiology. 2010; 254(3):837-845.
25. Cheng KY, Moazamian D, Ma Y, Jang H, Jerban S, Du J, et al. Clinical application of ultrashort echo time (UTE) and zero echo time (ZTE) magnetic resonance (MR) imaging in the evaluation of osteoarthritis. Skeletal Radiol. 2023.
26. Bae WC, Chen PC, Chung CB, Masuda K, D'Lima D, Du J. Quantitative ultrashort echo time (UTE) MRI of human cortical bone: correlation with porosity and biomechanical properties. J Bone Miner Res. 2012; 27(4):848-857.
27. Bae WC, Patil S, Biswas R, Li S, Chang EY, Statum S, et al. Magnetic resonance imaging assessed cortical porosity is highly correlated with muCT porosity. Bone. 2014; 66:56-61.

TABLES

Sequence	TR (ms)	TE (ms)	TSL (mm)	FA (deg)	BW (Hz)	ETL	Slice (mm)	FOV (mm)	Ph x Fr	Time (m:s)
3D FASE T1rho	1497	10	1, 16, 31, 46, 61, 76	90	651	162	3	220	320x320	2:12
3D UTE T1rho	3.7	0.096	1, 21, 41, 61	5	488	1	2	200	16000 proj	5:32
3D MAPSS T1rho	6.0	2.8	0, 10, 40, 80	20	391	1	3	230	192x192	2:32

Table 1. Scan parameters. All sequences used spin lock frequency of 250 Hz. Abbreviations are: repetition time (TR), echo time (TE), flip angle (FA), bandwidth (BW), echo train length (ETL), slice thickness (Slice), field of view (FOV), phase encoding (Ph), frequency encoding (Fr), milliseconds (ms), minutes (m), seconds (s).

		T1rho Values [ms]		
Sequence	**TSL [ms]**	**2% agarose**	**3%**	**4%**
3D FASE T1rho	1, 16, 31, 46, 61, 76	54.9	43.1	32.8
3D UTE T1rho	1, 21, 41, 61	45.8	39.1	29.0
3D MAPSS T1rho	1, 10, 40, 80	51.3	34.2	28.0

Table 2. T1rho values of agarose phantoms.

		AM	PM	FC	TC	ROI
3D FASE	mean (ms)	28.2	29.7	34.4	29.1	***p*=0.03**
	std (ms)	7.8	7.4	6.1	6.1	
	n	18	20	20	20	
3D UTE	mean (ms)	22.1	24.2	26.8	25.9	*p*=0.25
	std (ms)	10.1	5.2	7.6	7.3	
	n	20	20	20	20	
3D MAPSS	mean (ms)	24.7	26.7	37.9	35.9	***p*<0.001**
	std (ms)	5.1	7.6	2.6	3.9	
	n	12	12	12	12	

Table 3. T1rho values (mean and standard deviation, std, and number of regions, n) of cartilage and meniscus of human subjects. Abbreviations are: AM=anterior meniscus, PM=posterior meniscus, FC=femoral cartilage, TC=tibial cartilage, ROI=regions of interest.

FIGURE LEGENDS

Figure 1. Schematic of three T1rho pulse sequences used in this study. Each sequence has a (A) T1rho preparation pre-pulse followed by (B) 3D FASE, (C) 3D UTE, or (D) 3D MAPSS acquisitions. Three different readouts, (B) standard 3D FASE with a Cartesian trajectory, (C) 3D UTE with radial trajectory, and (D) 3D MAPSS with centric ky-kz trajectory are shown. Compared to (B) 3D FASE, (D) 3D MAPSS acquires from the center of k space without collecting periphery of k space, allowing shorter acquisition time. (C) UTE readout collects signal starting from the center of k space and the sampling become sparse in the periphery. Because of oversampling at the center of k space, UTE is not sensitive to motion artifacts. However, insufficient sampling causes streaking artifacts.

Figure 2. Agarose phantoms with 2%, 3%, and 4% were scanned with three T1rho sequences with (A) 3D FASE, (B) 3D UTE, and (C) 3D MAPSS acquisitions. Raw images at specific TSL and T1rho colormaps are shown. Colormaps from all sequences showed a trend of decreasing T1rho values with increasing agarose concentration.

Figure 3. T1rho relaxation curves for 2% agarose phantom, showing relatively tight fits.

Figure 4. (A, C, E) T1rho-weighted images at varying spin lock times (TSL) and (B, D, F) T1rho colormaps of a lateral compartment of a human knee acquired with (A, B) 3D FASE, (C, D) 3D UTE, and (E, F) 3D MAPSS T1rho sequences.

Figure 5. Bland-Altman plots comparing cartilage and meniscus T1rho values from (A) 3D MAPSS and 3D FASE, (B) 3D UTE and 3D FASE, and (C) 3D UTE and 3D MAPSS sequences. Note a very small bias between the T1rho values from 3D MAPSS and 3D FASE, and a large negative bias comparing T1rho values from 3D UTE to other two sequences.

FIGURES

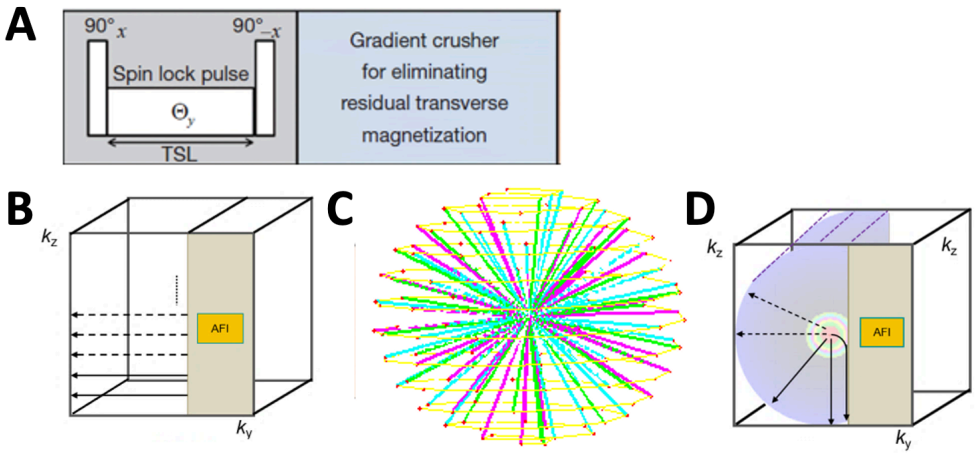

Figure 1. Schematic of three T1rho pulse sequences used in this study. Each sequence has a (A) T1rho preparation pre-pulse followed by (B) 3D FASE, (C) 3D UTE, or (D) 3D MAPSS acquisitions. Three different readouts, (B) standard 3D FASE with a Cartesian trajectory, (C) 3D UTE with radial trajectory, and (D) 3D MAPSS with centric ky-kz trajectory are shown. Compared to (B) 3D FASE, (D) 3D MAPSS acquires from the center of k space without collecting periphery of k space, allowing shorter acquisition time. (C) UTE readout collects signal starting from the center of k space and the sampling become sparse in the periphery. Because of oversampling at the center of k space, UTE is not sensitive to motion artifacts. However, insufficient sampling causes streaking artifacts.

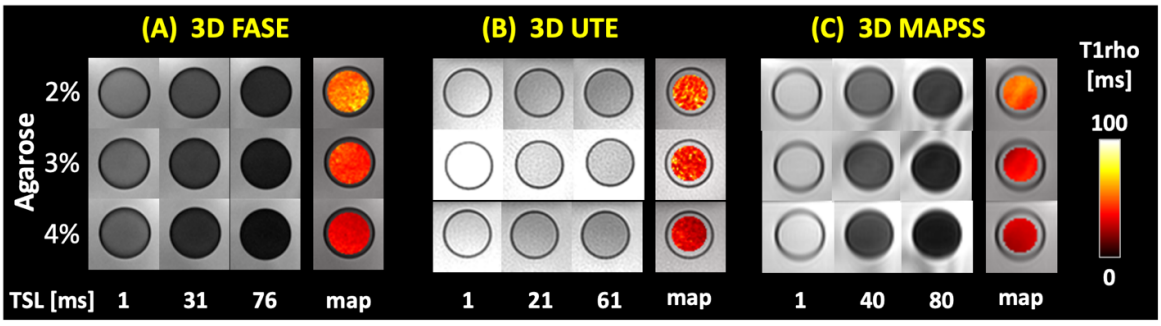

Figure 2. Agarose phantoms with 2%, 3%, and 4% were scanned with three T1rho sequences with (A) 3D FASE, (B) 3D UTE, and (C) 3D MAPSS acquisitions. Raw images at specific TSL and T1rho colormaps are shown. Colormaps from all sequences showed a trend of decreasing T1rho values with increasing agarose concentration.

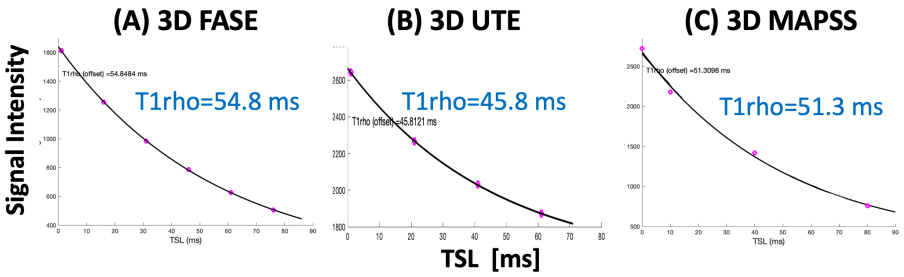

Figure 3. T1rho relaxation curves for 2% agarose phantom, showing relatively tight fits.

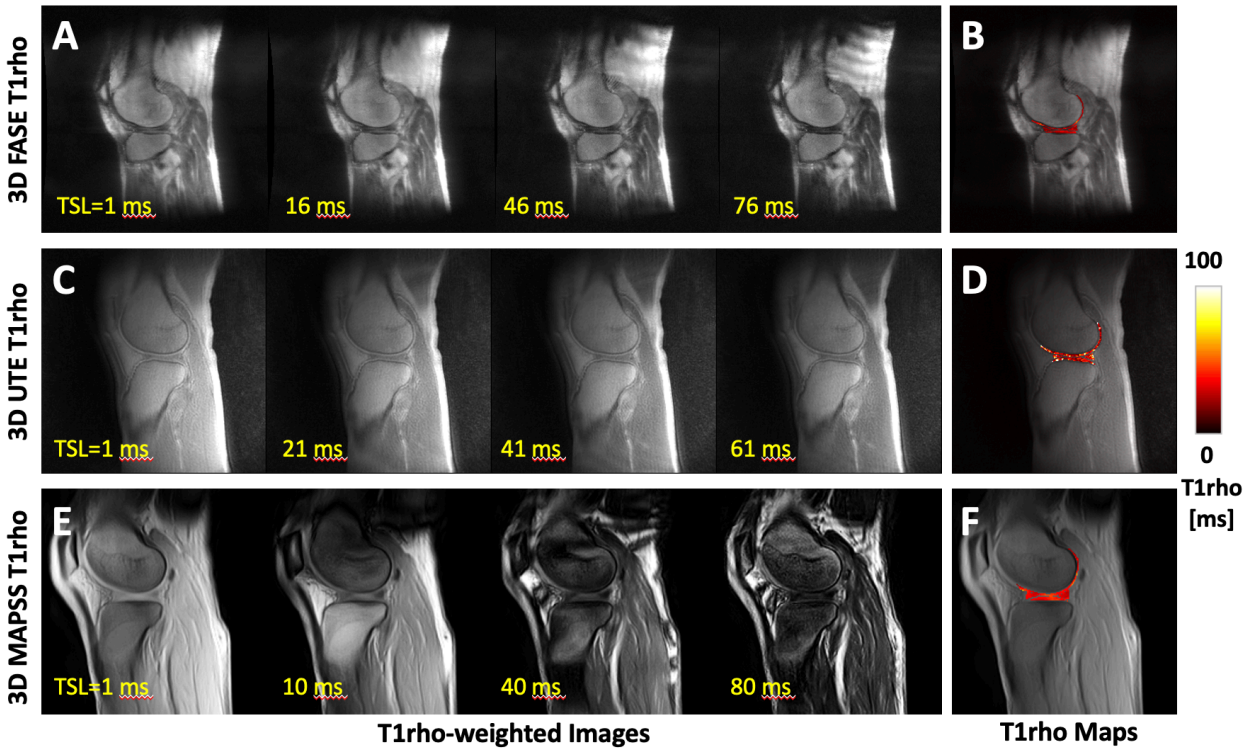

Figure 4. (A, C, E) T1rho-weighted images at varying spin lock times (TSL) and (B, D, F) T1rho colormaps of a lateral compartment of a human knee acquired with (A, B) 3D FASE, (C, D) 3D UTE, and (E, F) 3D MAPSS T1rho sequences.

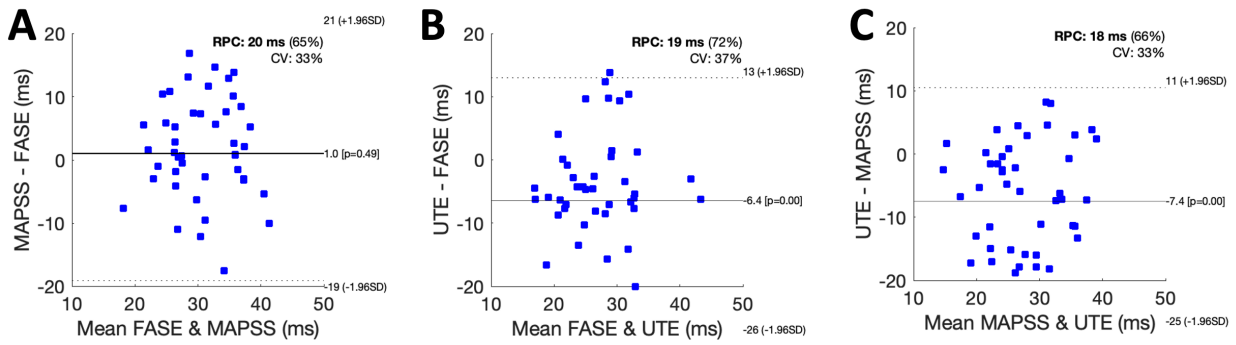

Figure 5. Bland-Altman plots comparing cartilage and meniscus T1rho values from (A) 3D MAPSS and 3D FASE, (B) 3D UTE and 3D FASE, and (C) 3D UTE and 3D MAPSS sequences. Note a very small bias between the T1rho values from 3D MAPSS and 3D FASE, and a large negative bias comparing T1rho values from 3D UTE to other two sequences.